Journal of The Electrochemical Society, **155** (8) H620-H624 (2008)
0013-4651/2008/155(8)/H620/5/$23.00 © The Electrochemical Society

Effect of Impurity and Illumination on Copper Oxidation after Chemical Mechanical Polishing

Hsien-Ping Feng,*,z Jeng-Yu Lin,* Yung-Yun Wang, and Chi-Chao Wan**

Department of Chemical Engineering, National Tsing-Hua University, Hsinchu 300, Taiwan

Copper-oxide defect is initiated at the grain boundary on the interconnect surface, and size increases with time and finally reaches a fixed value over a period of time after chemical mechanical polishing. The growth rate of copper oxide increases with increasing impurity content, resulting in more nucleation sites. Illumination significantly enhances and accelerates the growth rate at the initial nucleation stage by providing more electron carriers and acceptors for copper-oxide generation. Additionally, the nucleated reaction can be enhanced by illumination at the grain boundary with more sulfur content. Optical scan and X-ray photoelectron spectroscopy results prove that the illumination effect has a stronger correlation to sulfur than carbon or oxygen.
 [DOI: 10.1149/1.2946713]

Manuscript submitted March 24, 2008; revised manuscript received May 27, 2008. Available electronically June 27, 2008.

In copper damascene processes, chemical mechanical polishing (CMP) is applied to produce planarized copper lines with an intact surface. The presence of defects in the copper surface directly determines the interconnect qualities such as the adhesion of dielectric film, stress reliability, and the continuity of multilevel interconnection. Using the optical scan method, almost all the defect types, such as residues, water spots, pits, and scratches, can be detected just after polishing. These defects are related to polishing torque, slurry behavior, cleaning efficiency, and deposit structure.[1-3] To eliminate these defects, we need to produce deposits with stronger chemical resistance or control many parameters during CMP.[2,3] In addition to eliminating these defects resulting from plating or polishing processes, it is also important to prevent defects after CMP. Therefore, copper-interconnect surfaces must be kept in good condition after polishing and before dielectric-layer deposition. Generally, copper oxidation is a heterogeneous reaction which produces copper-oxide defects after polishing and before dielectric deposition. To minimize oxide defects, it commonly uses inhibitors or restricts the time from polishing to dielectric deposition. Some reports have studied a variety of inhibitors, such as benzotriazole (BTA), and their performance in retarding the oxidation rate.[4,5] Other reports have focused on how to erase copper oxide by in situ plasma or ammonia treatment prior to dielectric deposition.[6,7] However, few papers have discussed the phenomenon of copper-oxide defect after CMP. In this article, we propose an explanation of oxide formation on the copper-interconnect surface at the initial nucleation stage and under light illumination after CMP.

Experimental

Wafer preparation.— Patterned wafers with different line widths were generated by optical lithography and etching processes. This study used 12 in. Si(100) wafers with 100 nm thermal oxide/30 nm TaN/150 nm Cu seed layer/1000 nm copper deposit. TaN and Cu seed layers were deposited by physical vapor deposition without vacuum breaking. Electrodeposition was carried out with Novellus Sabre hardware using 15°C bath control and 180°C annealing (60 s). Electroplating studies were performed in an acid copper sulfate electrolyte containing 50 g/L copper metal, 200 g/L sulfuric acid, and 100 mg/L chloride ion. Two additives, 1 mL/L of a proprietary organic accelerator additive of the sulfide type [Shipley Company, similar to bis(3-sulfopropyl) disulfide] and 10 mL/L of a proprietary organic additive suppressor of the polyglycol type [Shipley Company, similar to poly(ethylene glycol)], were added to the electrolyte. An Applied-Material Mirra polisher was used to polish these wafers. Polishing conditions are head of 70 rpm, platen of 70 rpm, and down force of 2 psi. Two-step polishing processes were carried out, including the first stage for copper polishing and the second for Ta and oxide polishing. The copper polishing slurry was prepared with 3.1 wt % fumed aluminum particles and an acid solution at pH 3–5 containing 0.2 wt % hydrogen peroxide, 1 wt % passivation agent (BTA), and a phthalic acid salt that is commonly used in metal CMP slurries as a buffering and chelating agent. The peroxide and the passivation agent were used as the oxidizer and inhibitor for this study, respectively.

Measurement.— The optical scan method (KLA) was used to detect surface defects on the Cu film after CMP. The defect types were classified and determined with an AMAT SEMVISION reviewing tool. Impurities of the Cu surface were detected by secondary ion mass spectrometry (SIMS).

Light experiment.— Every patterned wafer was processed by the same plating and polishing process and placed in the same location of a clean room. Illumination used the same light source (300 W xenon lamp, Newport, wavelength 400–700 nm). All experiments were processed in a clean room. For experimentation, each wafer was used only one time for optical scanning and scanning electron microscopy (SEM) review. Then, each experiment was repeated three times to verify the repeatability of the results.

Results and Discussion

Figure 1 shows the SEM images of copper oxide defects growing on 0.2 μm lines at various time intervals. An interesting phenomenon is seen where the copper-interconnect surface generates copper-oxide defects randomly over a period of time after CMP. The size of copper-oxide defect increases with time and finally reaches a steady value. Figure 2 is an Auger analysis to detect a 0.2 μm line, comparing the copper surface with and without defect. It reveals that defects located at the Cu surface have more impurities (sulfur, carbon, and oxide). It is reasonable to infer that some increase of oxide content results from copper-oxide derivatives. Generally, grain boundaries cannot be seen clearly in SEM images; the narrow line (0.2 μm) is a bamboo structure, the grain boundaries of which are

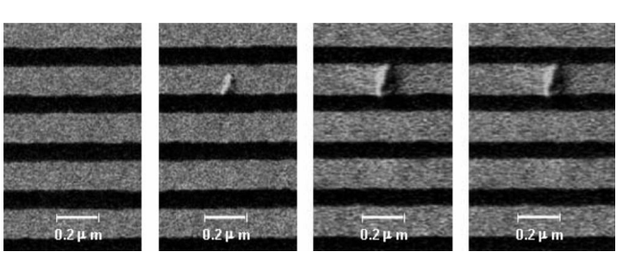

Figure 1. SEM images of copper-oxide defect on copper surface after polishing: (A) 2, (B) 8, (C) 24, and (D) 48 h after polishing.

* Electrochemical Society Student Member.
** Electrochemical Society Active Member.
z E-mail: nt-fong@hotmail.com

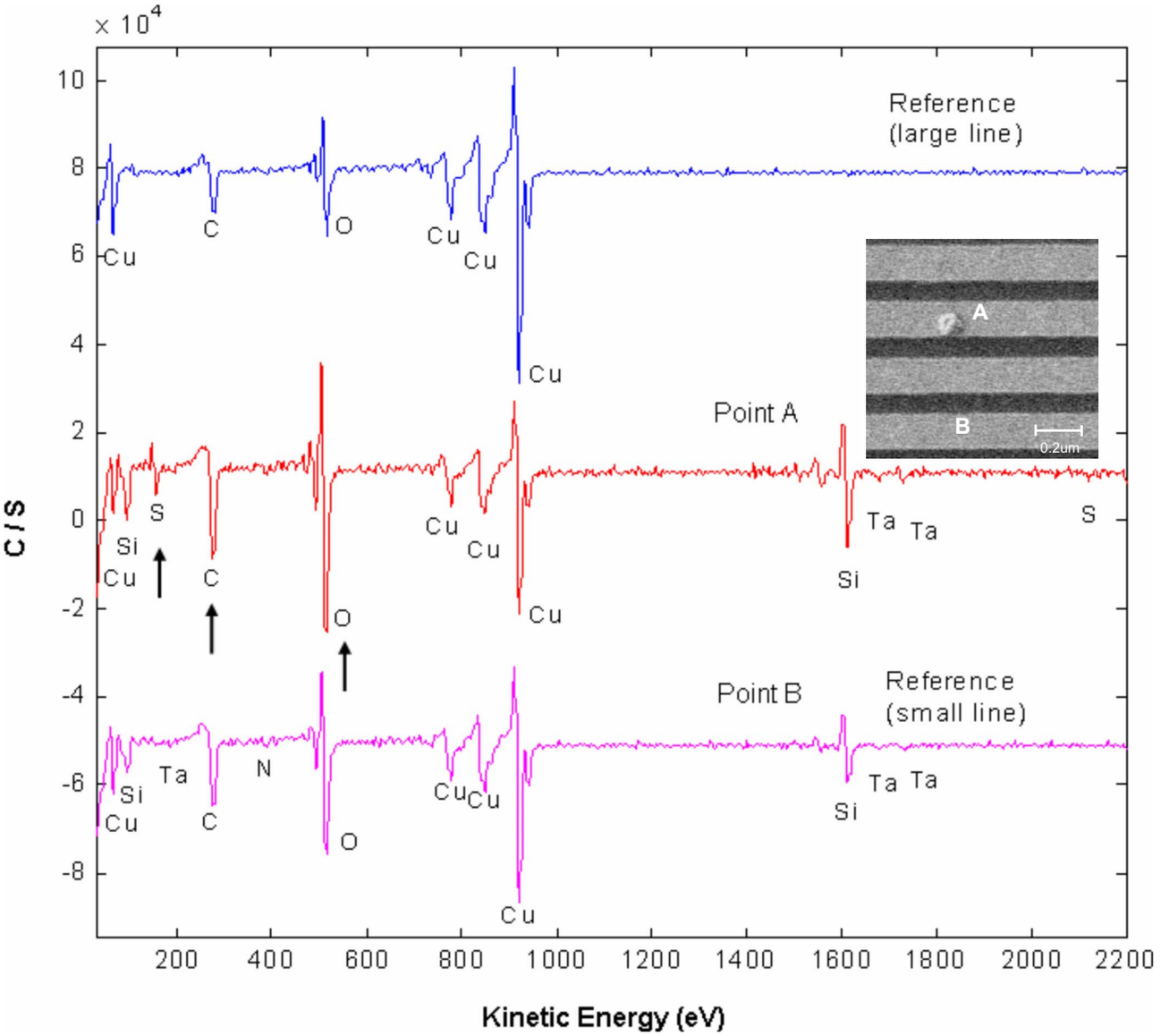

Figure 2. (Color online) Auger analysis for the location with and without defect on the copper-interconnect surface.

covered by oxide defects 0.15–0.2 μm in size. For this reason, copper-oxide defects located on the 1 μm wide line surface through 5 s HCl dipping are used to investigate surface morphology, and it is found that the defects are related to the properties of grain boundaries, as shown in Fig. 3. Moreover, Fig. 4 shows the experimental statistics for copper-oxide defects vs diverse linewidths, showing more copper-oxide defects in narrow lines (<0.3 μm) than in wide lines (>1 μm). According to metallurgical principles, impurities (sulfur, carbon, and oxide) that are derived from plating bath additives (accelerator and brightener) are concentrated at grain boundaries via postplating annealing.[8,9] Furthermore, it had been reported that the geometry effect causes high-level impurities to be trapped in narrower lines, which can lead to a correlation between impurity effect and the observation that narrow lines have more copper-oxide defects.[10,11] In 2002, a study by Thumer and Willams[11] on autocatalytic oxidation used observation by scanning tunneling microscopy to illustrate that metal-oxide grains nucleated readily at the exposed impurity sites (sulfur, carbon, and oxide). The initial stage is generally assumed to proceed via the formation of a chemisorbed O monolayer, followed by nucleation, growth, and coalescence of two-dimensional oxide islands. In summary, deposits with more impurities have high surface energy to generate more nucleation sites, resulting in more copper-oxide growth after CMP.

In addition to the impurity effect, it was found that illumination significantly enhances and accelerates the growth rate for copper-oxide generation, as shown in Fig. 5. Under illumination, copper-oxide defects are generated fast at the beginning of the reaction and gradually tend to stabilize, the number of which have no significant variation during 10 min, 60 min, or continuous illumination. This means that illumination influences the nucleation stage of copper-oxide growth for the most part. Therefore, the number of copper-oxide defects with illumination is obviously higher than that without illumination because of more nucleation sites. Mott and Cabrera were the first to point out the effect of light on oxidation and considered the modified band structure of the metal-oxide interface.[12-15] They suggested that the low mobility can be strongly enhanced by the contact potential produced by the electrons from the metal to the oxide surface at low temperatures. Recently, Chang and Ramanathan[16] presented a theoretical approach to investigate low-temperature nanoscale oxidation of metals. First, the metal/oxide

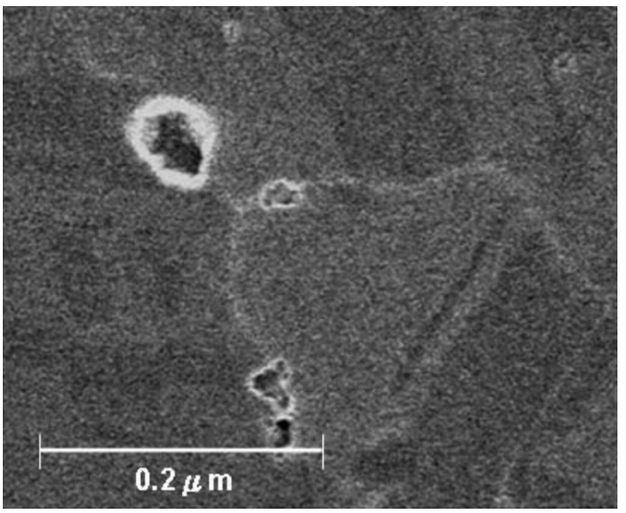

Figure 3. SEM image of copper-oxide defect on the copper surface after polishing 8 h (HCl dipping for 5 s to enhance grain boundaries).

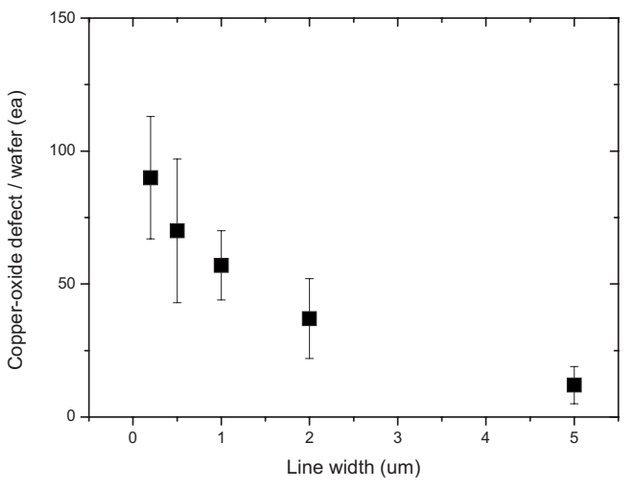

Figure 4. Copper-oxide defect vs line width after polishing 8 h.

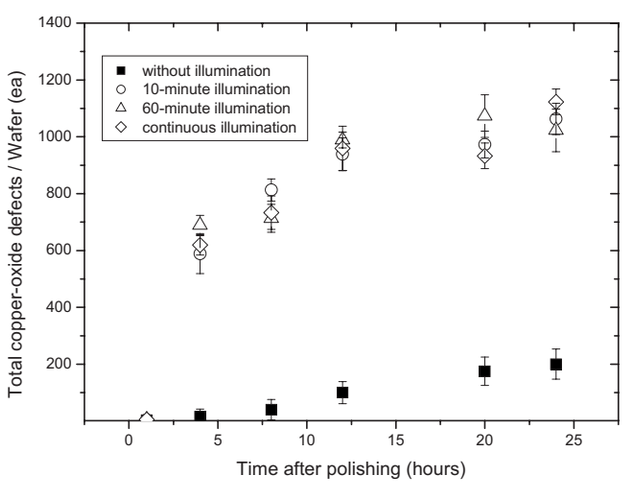

Figure 5. Copper-oxide defect vs time with and without illumination.

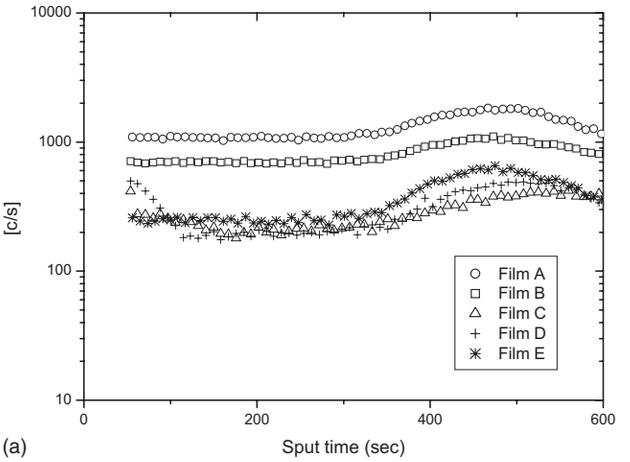

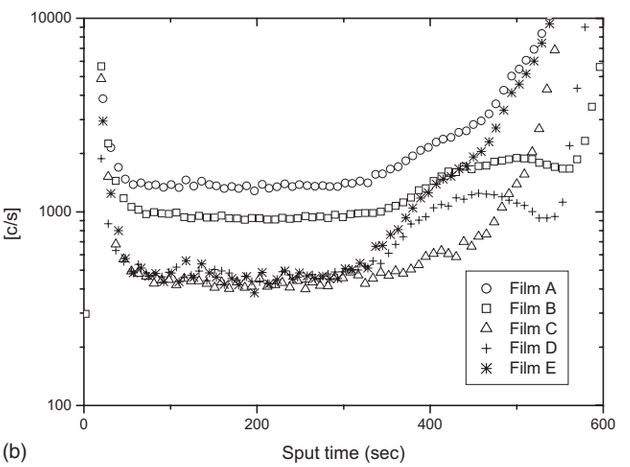

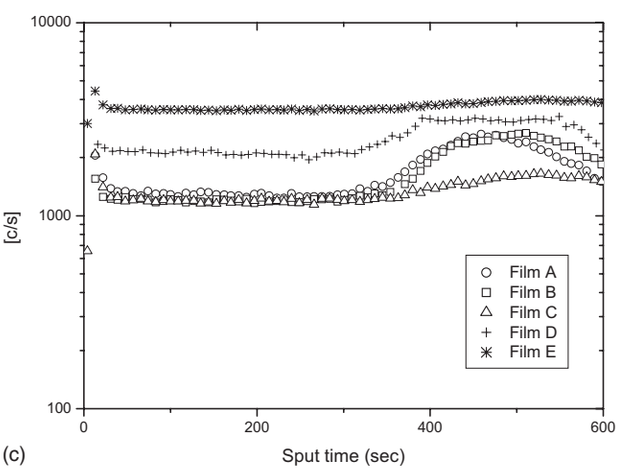

Figure 6. SIMS measurement of (a) carbon, (b) oxygen, and (c) sulfur for five deposits with different impurity contents (as listed in Table I).

interface is the reaction front, and for thin oxides, electrons tunnel through the oxide (tunnel current). During irradiation, electron currents are higher than in the normal oxidation condition. In the initial stage, these increased electron currents produce higher chemisorption density $\theta_O^-(\text{chem})$ on the oxide surface. The increased $\theta_O^-(\text{chem})$ raises the chemisorption level E_O^- above the Fermi level.[16,17] Electron transport reaches a steady state after the initial

Table I. List of film properties for five deposits with 20 mA/cm^2 and 1000 nm.

	Preparing method		XRD analysis		SIMS measurement[a]		
Film	Anneal temperature (°C)	Accel concentration (ml/L)	(111)/(200)	FWHM	Carbon	Oxide	Sulfur
A	180	1.0	5.83	0.573	1.60	3.95	1.03
B	200	1.0	5.79	0.578	1.00	1.00	1.00
C	220	1.0	5.81	0.575	0.35	0.59	0.94
D	220	3.0	5.78	0.580	0.38	0.54	1.78
E	220	5.0	5.83	0.577	0.39	0.55	2.31

[a] SIMS analysis results compared with film B as standard "1."

rapid growth region. Second, we consider the oxide/gas interface. Oxygen molecules are defined as weakly physisorbed, and then physisorbed oxygen species can act as electron acceptors for electrons from the metal to generate strong bonding chemisorption ions. Under the influence of light, not only O_2 but also O and O_3 impinge upon the oxide surface. O_3 is considered the supplier of O_2 and O, which indicates that there are sufficient electron acceptors O^- to accept the electrons originating from metal during radiation. According to this model, light illumination increases electron currents to produce higher chemisorption density θ_O^-(chem) on the copper-interconnect surface and generate more electron acceptors O^- to accept the electrons originating from copper. Thus, these two effects result in the initial rapid growth of copper-oxide extrusions as shown in Fig. 5. After that, the growth is slow because electron transport reaches a steady state, limiting the diffusion of tunneling electrons for a thicker film. In other words, light effect raises the driving force, which provides more electron carriers and acceptors for copper-oxide generation at the initial stage of nucleation on the copper-interconnect surface after polishing.

As mentioned above, nucleation sites are related to two effects, impurities of grain boundaries and illumination. Copper-oxide defects are generated heterogeneously at grain boundaries with high impurities because of high surface energy. Subsequently, the illumination enhances the probability that these locations will become the nucleation sites. Hence, we need to further understand the roles of impurities in detail. In general, desorption efficiency of impurities under heating differs due to diversity in bonding energy. According to previous studies,[18] the Cu–S bonding (276 KJ/mol) is too stable to be removed by annealing. As the Cu–C bonding is weak (9.8 KJ/mol), carbon is expected to separate from Cu film through annealing. So, carbon content is supposed to be reduced by increasing thermal energy. Moreover, the bonding strength of Cu–O (269 KJ/mol) is reported to be almost identical to that of Cu–S (276 KJ/mol), implying that this thermal energy cannot break the Cu–O bonding. Liu et al.[18] prove that O atoms bonded to C can coevaporate with C in the form of CO_x and that, bonded to Cu, will be trapped like S. It is believed that O atoms are randomly distributed to copper as deposited. After annealing, some form the remaining Cu–O and others form CO_x, reducing oxygen incorporation in the films. Distinguishing between the Cu–O and the Cu–CO_x bonding effects is difficult at this point, but O also decreases with increasing thermal energy. Briefly, annealing can release C and O from the plated films, while S strongly bonds in the films. Therefore, increasing anneal temperature can reduce carbon/oxide and keep the same sulfur content. Furthermore, sulfur can be derived from adding various accelerator concentrations in the plating bath, which causes various amounts of sulfur to remain in the deposits, and carbon/oxide can be reduced to low levels after anneal treatment. As above, in order to understand the relationship between impurities and illumination, we made five deposits with different impurity contents by changing the anneal temperature and accelerator-additive amount. Figures 6a-c are the SIMS results for these deposits, including sulfur, carbon, and oxide. Additionally, X-ray diffraction (XRD) analysis shows identical levels for (111)/(200) ratio and full width at half-maximum (fwhm), meaning orientation and grain size are not changed by these conditions. Table I summarizes experimental conditions, film structures, and impurity contents for these five deposits. Based on Table I, the impact of carbon and oxygen can be estimated among films A, B, and C, and sulfur effect can be determined by films C, D, and E.

Subsequently, optical scanning with SEM review is used to evaluate copper-oxide defects over 24 h after polishing, and Cu ($2p_{3/2}$) and O (1s) X-ray photoelectron spectroscopy (XPS) is used to derive the oxide/Cu ratio, as seen in Fig. 7. According to XPS and reviewed defect data, the growth rate of copper-oxide increases with increasing sulfur content but does not change with carbon and oxide content, indicating that Cu surfaces with more sulfur induce fast oxide growth under illumination. In addition, Cu et al. reported that oxide growth occurs slowly on the S-free Cu surface as compared with the S-modified copper surface.[19] Although they focused on the homogeneous bulk Cu surface in solution and did not bring up the illumination effect, it can provide additional evidence for the relationship between copper-oxide generation and sulfur content.

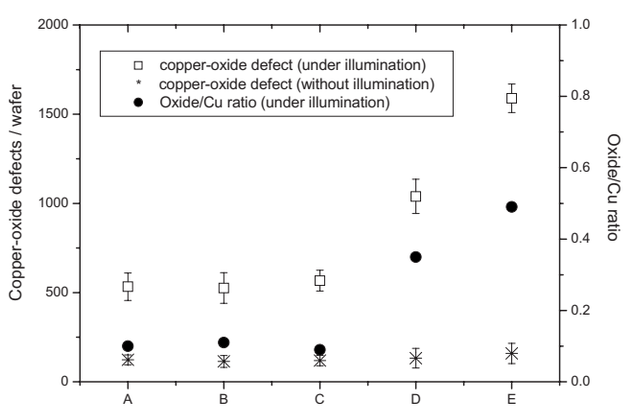

Figure 7. Copper-oxide defect and XPS oxide/Cu ratio for deposits with different impurity contents over 24 h after polishing under illumination.

Conclusions

Impurities of grain boundaries act as nucleation sites to generate copper-oxide defect, which continues to grow and coalesce after CMP. The growth rate of copper-oxide defect first increases quickly and then slows as a result of the diffusion limitation of tunneling electrons from copper to the oxide film. Illumination causes abrupt nucleated growth because it produces higher chemisorption density, raising the potential difference. Nucleated reaction of copper oxide is enhanced by illumination when the grain boundary has sufficient sulfur. Additionally, the presence of carbon or oxygen in the grain boundary does not seem to influence the copper-oxide growth rate.

National Tsing Hua University assisted in meeting the publication costs of this article.

References

1. K.-W. Chen and Y. L. Wang, *J. Electrochem. Soc.*, **154**, H41 (2007).
2. K. W. Chen, Y. L. Wang, L. Chang, S. C. Chang, F. Y. Li, and S. H. Lin, *Electrochem. Solid-State Lett.*, **7**, G238 (2004).
3. H.-P. Feng, J.-Y. Lin, M.-Y. Cheng, Y.-Y. Wang, and C.-C. Wan, *J. Electrochem. Soc.*, **155**, H21 (2008).
4. A. T. Al-Hinai and K. Osseo-Asare, *Electrochem. Solid-State Lett.*, **6**, B23 (2003).
5. Y.-K. Hong, D.-H. Eom, S.-H. Lee, T.-G. Kim, J.-G. Park, and A. A. Busnaina, *J. Electrochem. Soc.*, **151**, G756 (2004).
6. Y. Jin, K. Kondo, Y. Suzuki, T. Matsumoto, and D. P. Barkey, *Electrochem. Solid-State Lett.*, **8**, C6 (2005).
7. G. A. Hope and R. Woods, *J. Electrochem. Soc.*, **151**, C550 (2004).
8. M. Tan and J. N. Harb, *J. Electrochem. Soc.*, **150**, C420 (2003).
9. Q. T. Jiang and M. E. Thomas, *J. Vac. Sci. Technol. B*, **B19**, 762 (2001).
10. W. Zang, *J. Electrochem. Soc.*, **152**, C832 (2005).
11. K. Thurmer, E. Williams, and J. Rutt-Robey, *Science*, **297**, 2033 (2002).
12. N. F. Mott, *Trans. Faraday Soc.*, **35**, 1175 (1939).
13. N. F. Mott, *Trans. Faraday Soc.*, **36**, 472 (1940).
14. N. F. Mott, *Trans. Faraday Soc.*, **43**, 431 (1947).
15. N. Cabrera and N. F. Mott, *Rep. Prog. Phys.*, **12**, 163 (1949).
16. C.-L. Chang and S. Ramanathan, *J. Electrochem. Soc.*, **154**, G160 (2007).
17. A. T. Fromhold, Jr., *Theory of Metal Oxidation*, Vol. 1, *Fundamentals*, p. 250, North-Holland, Amsterdam (1976).
18. C.-W. Liu, Y.-L. Wang, M.-S. Tsai, H.-P. Feng, S.-C. Chang, and G.-J. Hwang, *J. Vac. Sci. Technol. A*, **23**, 658 (2005).
19. H.-C. Cu, G. Seshadri, and J. A. Kelber, *J. Electrochem. Soc.*, **147**, 558 (2000).